

# Mathematics and Mechanics of Solids

<http://mms.sagepub.com>

---

## **Analysis of Shaft-Loaded Membrane Delamination Using Stationary Principles**

Carmel Majidi, Richard E. Groff and Ron S. Fearing

*Mathematics and Mechanics of Solids* 2008; 13; 3 originally published online Jan 31, 2007;

DOI: 10.1177/1081286506068823

The online version of this article can be found at:  
<http://mms.sagepub.com/cgi/content/abstract/13/1/3>

---

Published by:



<http://www.sagepublications.com>

**Additional services and information for *Mathematics and Mechanics of Solids* can be found at:**

**Email Alerts:** <http://mms.sagepub.com/cgi/alerts>

**Subscriptions:** <http://mms.sagepub.com/subscriptions>

**Reprints:** <http://www.sagepub.com/journalsReprints.nav>

**Permissions:** <http://www.sagepub.co.uk/journalsPermissions.nav>

**Citations** <http://mms.sagepub.com/cgi/content/refs/13/1/3>

# Analysis of Shaft-Loaded Membrane Delamination Using Stationary Principles

CARMEL MAJIDI

RICHARD E. GROFF

RON S. FEARING

*Department of Electrical Engineering & Computer Science University of California  
Berkeley, CA 94720, USA*

(Received 24 January 2006; accepted 20 June 2006)

*Abstract:* The following analysis investigates the delamination of an elastic membrane which on one side adheres to a smooth substrate while the other side is attached to a rigid cylindrical shaft. When the shaft is pulled perpendicularly from the substrate, this system is equivalent to the blister test of Malyshev and Salganik (*International Journal of Fracture Mechanics*, 1, 114 (1965)) and a solution is derived using the principle of minimum potential energy. Delamination can also be caused by rotating the shaft, which may be induced by a shear load and/or moment applied to the free end. For this more complicated system, an approximate solution is obtained from upper and lower bounds on strain energy that are derived from stationary principles with restricted deformation and stress fields, respectively. Beyond their applicability to blister tests, these results are relevant to the emerging study of biologically-inspired adhesives, as membranes constitute a critical attachment structure for a variety of wall-clinging organisms.

*Key Words:* Non-linear membrane theory, stationary principles, complementary energy, Hencky strain measure

## 1. INTRODUCTION

A shaft-loaded membrane, such as the one illustrated in Figure 1, may be detached from a substrate either by pulling the shaft perpendicularly from the substrate (equivalent to the blister test of [1]) or by rotating the shaft about the substrate plane. Systems related to the normal pull-off mode have been studied [2, 3] and are relevant to applications ranging from MEMS devices [4] to intracellular binding [5]. There has also been recent interest in the role of shaft-supported thin plates found in the adhesive system of wall climbing geckos [6, 7, 8, 9] (more general information on gecko adhesion can be found in the popular literature [10, 11]). Each plate, known as a *spatula*, has a thickness of 5–10 nanometers and is connected along one edge to a terminal branch of the shaft, known as a *seta*. The spatulae, due to their thin geometry, can achieve intimate contact with a micro-rough surface with little elastic strain and thus adhere through short-range van der Waals attraction [12]. Because they are

*Mathematics and Mechanics of Solids* **13**: 3–22, 2008

©SAGE Publications 2008

Los Angeles, London, New Delhi and Singapore

DOI: 10.1177/1081286506068823

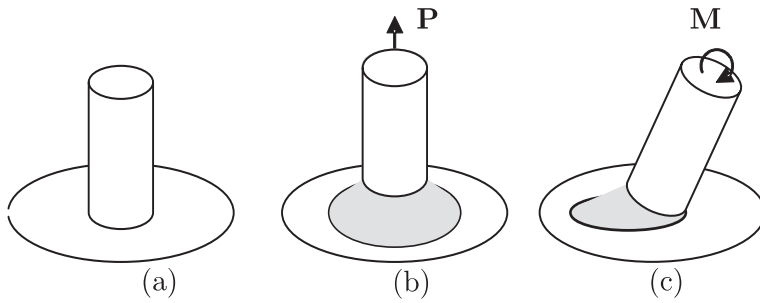


Figure 1. Illustration of shaft loaded membrane; (a) reference configuration, (b) delamination under normal translation, (c) delamination under rotation.

supported at one edge, however, gecko spatulae peel easily under normal loading, following the Kendall peel model [9, 13]. For a synthetic bio-inspired adhesive with high normal load resistance, we propose a symmetric structure wherein the membrane-like spatula is connected to the supporting shaft at its center rather than along its edge. The following analysis presents the governing equations necessary to predict the detachment resistance to both normal and moment loading of the proposed design.

Here we consider an isotropic elastic membrane sheet that is connected at its center to a rigid cylindrical shaft. For normal pull-off, the delamination zone is axisymmetric and can be parameterized by radius alone, allowing the computation of a strain energy release rate [2]. If delamination is generated by shaft rotation, however, its shape must be identified by a real-valued function, significantly complicating the analysis. For this loading condition, it is convenient to consider only a restricted set of kinematically admissible deformation fields and statically admissible stress fields. Applying the stationary principles presented in [14] then yields upper and lower bounds for the strain energy functional. This method employs the principle of maximum complementary energy, a technique that has been applied to other problems in non-linear membrane theory, including the study of a clamped circular membrane that sags under its own weight [15, 16], the axial extension of a cylindrical membrane [14], and the puncturing of a thin elastic sheet [17]. For detailed derivation and discussion of the principle of maximum complementary energy, the interested reader should refer to sections in [18, 19, 20].

Here we adopt the classical strain-energy function of infinitesimal isotropic elasticity. To allow the theory to be valid for moderately large deformations, the infinitesimal strains are replaced by the Hencky (logarithmic) measure for finite strain [21, 22]. In the case of delamination by shaft rotation, it is demonstrated that for the geometry and loading range of interest, a similar result can be obtained with the Green strain.

An overview of the governing equations and principles for the shaft-loaded membrane are presented in Section 2. This includes a summary of the kinematics and constitutive law, as well as a discussion on the stationary principles of minimum potential and maximum complementary energy. Next, these principles are applied to the delamination of the shaft-loaded membrane. An approximate solution is derived for the case of delamination under shaft rotation. Numerical results are presented for both systems in Section 5. For delamination under

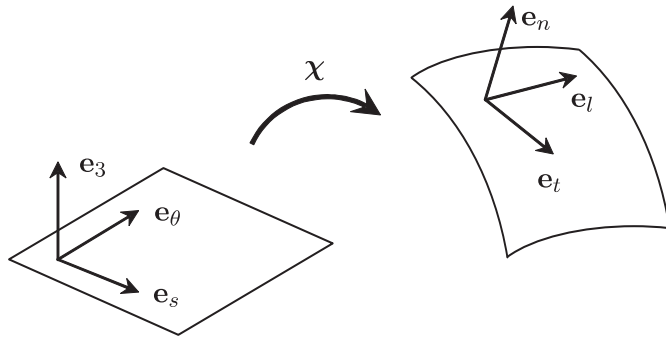


Figure 2. Local coordinate system in reference and deformed configurations.

rotation, the solution accuracy is demonstrated by the tightness in the bounds furnished by the two variational methods.

## 2. GOVERNING EQUATIONS

Let  $\mathcal{S}$  represent the surface of a rigid, infinite half-space and define the right-handed orthonormal triad  $\{\mathbf{e}_1, \mathbf{e}_2, \mathbf{e}_3\}$  such that  $\mathbf{e}_3$  is normal to the half-space. Next, let  $\mathbf{X} = X_1\mathbf{e}_1 + X_2\mathbf{e}_2 + X_3\mathbf{e}_3$  denote the position of any point in  $\mathbb{R}^3$  with respect to the origin  $O \in \mathcal{S}$ . In addition, let  $\{s, \theta, X_3\}$  represent a cylindrical coordinate system with origin  $O$  and polar axis  $\mathbf{e}_1$  and define the right-handed orthonormal triad  $\{\mathbf{e}_s, \mathbf{e}_\theta, \mathbf{e}_3\}$  such that

$$\mathbf{e}_s = \cos\theta\mathbf{e}_1 + \sin\theta\mathbf{e}_2 \quad \text{and} \quad \mathbf{e}_\theta = \mathbf{e}_3 \times \mathbf{e}_s. \quad (1)$$

The two coordinate systems are related by the equations

$$X_1 = s \cos\theta \quad \text{and} \quad X_2 = s \sin\theta. \quad (2)$$

Consider an homogeneous, elastic membrane that on one side adheres to the half-space and on the other side is attached to the base  $\mathcal{B}_0$  of a rigid cylindrical shaft. Delamination is possible by translating and/or rotating the shaft base to a new configuration  $\mathcal{B}$ . Let  $\Omega$  denote the midplane of the delaminated portion of the membrane that is not in contact with the shaft and identify its boundary  $\partial\Omega$  with the function  $v(\theta) \geq \rho \forall \theta \in [0, 2\pi]$  through the representation

$$\partial\Omega = \{\mathbf{X} \in \mathbb{R}^3 : s \in \{\rho, v(\theta)\}, \theta \in [0, 2\pi]\}. \quad (3)$$

The function  $v(\theta)$ , which defines the amount of delaminated material, may also be used to define the surface  $\Omega$  in its natural configuration:

$$\Omega_0 = \{\mathbf{X} \in \mathbb{R}^3 : s \in [\rho, \nu(\theta)], \theta \in [0, 2\pi], X_3 = 0\}. \quad (4)$$

### 2.1. Kinematics

Let the function  $\mathcal{X} : \Omega_0 \rightarrow \Omega$  map a point  $\mathbf{X} \in \Omega_0$  to its position  $\mathbf{x}$  in the deformed configuration  $\Omega$ , i.e.

$$\mathbf{x} = \mathcal{X}(\mathbf{X}) \quad \text{for} \quad \mathbf{X} \in \Omega_0. \quad (5)$$

Membrane theory assumes that there is no shearing along the tangent plane, and so the deformation may be expressed as

$$\mathcal{X}(\mathbf{X}) = \mathbf{X} - X_3 \mathbf{e}_3 + \mathbf{u}_0 + (X_3 + q) \mathbf{e}_n \quad (6)$$

where  $\mathbf{u}_0 = \mathbf{u}_0(s, \theta, X_3)$  is the displacement of a point on the midplane  $\Omega_0$ ,  $\mathbf{e}_n$  is the unit normal to the deformed surface  $\Omega$  and  $q = q(s, \theta, X_3)$  is the displacement of points away from the midplane relative to the deformed orientation. By definition of midplane, the function  $q$  vanishes identically on the midplane, and thus must satisfy the following conditions:

$$q(X_3 = 0) = \left( \frac{\partial q}{\partial s} \right)_{X_3=0} = \frac{1}{s} \left( \frac{\partial q}{\partial \theta} \right)_{X_3=0} = 0. \quad (7)$$

Consider the vectors

$$\mathbf{e}'_s = \mathbf{e}_s + \frac{\partial}{\partial s} \mathbf{u}_0 \quad \text{and} \quad \mathbf{e}'_\theta = \mathbf{e}_\theta + \frac{1}{s} \frac{\partial}{\partial \theta} \mathbf{u}_0, \quad (8)$$

which span the plane tangent to  $\Omega$ . These vectors are, in general, not perpendicular or of unit length but, nonetheless, can be used to evaluate the unit normal in the following way:

$$\mathbf{e}_n = \frac{\mathbf{e}'_s \times \mathbf{e}'_\theta}{\|\mathbf{e}'_s \times \mathbf{e}'_\theta\|}, \quad (9)$$

where  $\|\bullet\|$  is the Euclidean norm.

Define  $\mathbf{F} = \nabla \mathcal{X}(\mathbf{X})$  to be the gradient<sup>1</sup> of the deformation  $\mathbf{X} \mapsto \mathcal{X}(\mathbf{X})$ . This may be represented as

$$\mathbf{F}(\mathbf{X}) = \mathbf{F}_0 + \hat{\mathbf{F}} \quad (10)$$

where

$$\mathbf{F}_0 := \mathbf{F}(\mathbf{X} : X_3 = 0) = \mathbf{I} - \mathbf{e}_3 \otimes \mathbf{e}_3 + \nabla \mathbf{u}_0 + \left\{ 1 + \frac{\partial q}{\partial X_3} \right\} \mathbf{e}_n \otimes \mathbf{e}_3 \quad (11)$$

and

$$\hat{\mathbf{F}} := \mathbf{F} - \mathbf{F}_0 = (X_3 + q) \left\{ \frac{\partial \mathbf{e}_n}{\partial s} \otimes \mathbf{e}_s + \frac{1}{s} \frac{\partial \mathbf{e}_n}{\partial \theta} \otimes \mathbf{e}_\theta \right\} + \frac{\partial q}{\partial s} \mathbf{e}_n \otimes \mathbf{e}_s + \frac{1}{s} \frac{\partial q}{\partial \theta} \mathbf{e}_n \otimes \mathbf{e}_\theta. \quad (12)$$

By the polar decomposition theorem, there exists tensors  $\mathbf{R} \in \text{Orth}^+$  and  $\mathbf{V} \in \text{Sym}$  such that  $\mathbf{F} = \mathbf{VR}$ . The tensor  $\mathbf{V}$  is known as the left stretch tensor and its natural log is defined as the spatial Hencky strain tensor  $\mathbf{E}_H = \ln \mathbf{V}$ . The strain tensor may also be expressed as

$$\mathbf{E}_H = \frac{1}{2} \ln \mathbf{B} \quad (13)$$

where  $\mathbf{B} = \mathbf{FF}^T$  is the left Cauchy–Green tensor [23].

## 2.2. Stress Tensors and Constitutive Law

For moderately large deformations, the constitutive response of a material can be accurately characterized by a strain-energy function  $W(\mathbf{F})$  of the form

$$W = \mu(\gamma_I^2 + \gamma_{II}^2 + \gamma_{III}^2) + \frac{1}{2} \lambda (\gamma_I + \gamma_{II} + \gamma_{III})^2 \quad (14)$$

where  $\{\gamma_i : i = I, II, III\}$  are the eigenvalues of  $\mathbf{E}_H$  and  $\mu$  and  $\lambda$  are the Lamé moduli evaluated at small strains [21, 22]. Hencky's constitutive equation is given by

$$s_i = \frac{\partial W}{\partial \gamma_i} = 2\mu \gamma_i + \lambda (\gamma_I + \gamma_{II} + \gamma_{III}) \quad (15)$$

where  $\{s_i\}$  are the principal components (eigenvalues) of the Kirchhoff stress tensor  $\mathbf{S}$ . For plane stress problems, (14) reduces to

$$W = \frac{2\mu}{\lambda + 2\mu} [\lambda \gamma_t \gamma_l + (\lambda + \mu)(\gamma_t^2 + \gamma_l^2)] \quad (16)$$

where  $\gamma_t$  and  $\gamma_l$  are the principal strains on the tangent plane and

$$\gamma_n = -\frac{\lambda}{\lambda + 2\mu} (\gamma_t + \gamma_l) \quad (17)$$

is the principal strain normal to  $\Omega$ .

In tensorial form,

$$\mathbf{S} = 2\mu \mathbf{E}_H + \lambda (\text{tr} \mathbf{E}_H) \mathbf{1} \quad (18)$$

where  $\mathbf{1}$  is the unit tensor [21]. Inverting<sup>2</sup> (18) yields

$$\mathbf{E}_H = \frac{1}{2\mu} \left[ \mathbf{S} - \frac{\lambda}{2\mu + 3\lambda} (\text{tr}\mathbf{S})\mathbf{1} \right], \tag{19}$$

which implies

$$\gamma_i = \frac{1}{2\mu} s_i - \frac{\lambda}{(2\mu)(2\mu + 3\lambda)} (s_I + s_{II} + s_{III}). \tag{20}$$

Similarly, the strain energy function can be expressed as

$$W = W(\mathbf{F}) = \frac{1}{2} \mathbf{S} \cdot \mathbf{E}_H \tag{21}$$

$$= \hat{W}(\mathbf{E}_H) = \mu \text{tr}(\mathbf{E}_H^2) + \frac{1}{2} \lambda (\text{tr}\mathbf{E}_H)^2 \tag{22}$$

$$= \tilde{W}(\mathbf{S}) = \frac{1}{4\mu} \text{tr}(\mathbf{S}^2) - \frac{\lambda}{(4\mu)(2\mu + 3\lambda)} (\text{tr}\mathbf{S})^2. \tag{23}$$

Another stress tensor that will be relevant to analysis is the Piola tensor  $\mathbf{P} = \mathbf{F}^{-1}\mathbf{S}$ . Let  $\{\eta_i : i = I, II, III\}$  denote the eigenvalues of  $\mathbf{P}\mathbf{P}^T$ . Then, the principal components of  $\mathbf{P}$  are  $t_i = \sqrt{\eta_i}$ , which are known as the Biot stresses. For plane stress,

$$\gamma_t = \frac{1}{2\mu} t_t - \frac{\lambda}{(2\mu)(2\mu + 3\lambda)} (t_t + t_l) \tag{24}$$

$$\gamma_l = \frac{1}{2\mu} t_l - \frac{\lambda}{(2\mu)(2\mu + 3\lambda)} (t_t + t_l). \tag{25}$$

### 2.3. Membrane Approximation

For the applications presented in Sections 3 and 4, we consider a membrane of thickness  $H$ . For simplicity, it is assumed that  $H$  is vanishingly small. Thus, the deformation tensor is approximated by  $\mathbf{F}_m$ , which is defined as

$$\mathbf{F}_m := \lim_{H \rightarrow 0} \mathbf{F} \tag{26}$$

for all points in the membrane. Noting that  $|X_3| \leq 2H$  and  $H \rightarrow 0$ , it follows from (7) that

$$\mathbf{F}_m = \mathbf{F}_0 \equiv \mathbf{I} - \mathbf{e}_3 \otimes \mathbf{e}_3 + \nabla \mathbf{u}_0 + \left\{ 1 + \frac{\partial q}{\partial X_3} \right\} \mathbf{e}_n \otimes \mathbf{e}_3. \tag{27}$$

Based on this assumption of an infinitesimally thin membrane, the Hencky strain tensor becomes

$$\mathbf{E}_m = \frac{1}{2} \ln (\mathbf{F}_m \mathbf{F}_m^T). \quad (28)$$

Henceforth,  $\mathbf{F}_m$  and  $\mathbf{E}_m$  will be used in place of the deformation gradient and Hencky strain tensors, respectively.

#### 2.4. Variational Principles

For a prescribed shaft configuration  $\mathcal{B}$  and delamination zone  $\Omega_0$ , the total potential energy of the system is [14]

$$U(\chi) = \int_{\Omega_0} W H \, dA - \int_{\partial\Omega_0^\sigma} \boldsymbol{\sigma} \cdot \boldsymbol{\chi} H \, dS. \quad (29)$$

where  $\partial\Omega_0^\sigma$  denotes the part of the boundary where traction is prescribed and  $\boldsymbol{\sigma} = \mathbf{P}^T \mathbf{N}$  on  $\partial\Omega_0^\sigma$ . It should be noted that the work of adhesion (or surface energy) is not included in the potential energy, but will be introduced later. The dual to the potential is the complementary energy:

$$\Phi(\mathbf{P}) = \int_{\partial\Omega_0^x} (\mathbf{P}^T \mathbf{N}) \cdot \boldsymbol{\xi} H \, dS - \int_{\Omega_0} W_c H \, dA, \quad (30)$$

where  $\partial\Omega_0^x$  is the part of  $\partial\Omega_0$  where position is prescribed,  $\mathbf{N}$  is the unit outward normal to  $\partial\Omega_0^x$  lying in the tangent plane to  $\Omega_0$ ,  $\boldsymbol{\xi}$  is the prescribed position of points on  $\partial\Omega_0^x$ , and

$$W_c = \mathbf{P} \cdot \mathbf{F} - W \quad (31)$$

is the complementary energy density [17]. Assuming plane stress,  $W_c$  reduces to [14]

$$W_c = e^{\gamma_t} t_t + e^{\gamma_l} t_l - W. \quad (32)$$

where  $e^{\gamma_t}$  and  $e^{\gamma_l}$  are the principal stretches associated with eigenvalues of the Hencky strain tensors.

Let  $\mathcal{F}$  denote the space of all geometrically admissible deformation fields and define

$$\mathcal{P} := \{\mathbf{P} : \text{Div } \mathbf{P} = \mathbf{0}, \mathbf{P}^T \mathbf{N} = \boldsymbol{\sigma} \text{ on } \partial\Omega_0^\sigma\} \quad (33)$$

where Div is the divergence operation with respect to  $\mathbf{X}$ . At equilibrium, the potential energy is computed as

$$U^* = \min_{\chi \in \mathcal{F}} U(\chi) = \max_{\mathbf{P} \in \mathcal{P}} \Phi(\mathbf{P}). \quad (34)$$

To obtain an analytic solution, it may be convenient to study only a restricted class of deformation and stress fields, denoted by  $\mathcal{F}_0 \subset \mathcal{F}$  and  $\mathcal{P}_0 \subset \mathcal{P}$ , respectively. Extremizing over these restricted spaces will yield upper and lower bounds on  $U^*$ , respectively:

$$\min_{\chi \in \mathcal{F}_0} U(\chi) \geq U^* \geq \max_{\mathbf{P} \in \mathcal{P}_0} \Phi(\mathbf{P}). \tag{35}$$

Next, let  $W_s$  denote the work required to create new surface via delamination and define the total energy of the system as  $E = U + W_s$ . The work  $W_s$  may be expressed as

$$W_s = \int_{\Omega_0} W_{ad} \, dA, \tag{36}$$

where  $W_{ad}$  is the work of adhesion per unit area. By the Griffith energy balance,  $E$  is stationary with respect to variations of the form

$$v \mapsto \tilde{v} = v + \delta v, \tag{37}$$

where  $\delta v = \delta v(\theta)$  is an arbitrarily small but kinematically admissible perturbation of the field  $v(\theta)$ .

### 3. APPLICATION TO NORMAL PULL-OFF

Suppose that the shaft is pulled from the substrate through a distance  $\Delta$  such that

$$\mathbf{x} = \rho \mathbf{e}_s + \Delta \mathbf{e}_3 \tag{38}$$

for points on  $\partial \mathcal{B}$ . The deformation response is assumed to be axisymmetric, and so

$$\mathbf{u}_0 = u_s(s) \mathbf{e}_s + u_3(s) \mathbf{e}_3. \tag{39}$$

Following from (8) and (9),

$$\mathbf{e}_n = \frac{1}{\sqrt{(1 + u_{s,s})^2 + u_{3,s}^2}} \{-u_{3,s} \mathbf{e}_s + (1 + u_{s,s}) \mathbf{e}_3\}, \tag{40}$$

where  $u_{x,y} = \partial u_x / \partial y$ . Substituting these into the deformation gradient tensor (27) and then performing an eigen decomposition on the Hencky strain tensor (28) for points on the midplane yields

$$\mathbf{E}_m = \gamma_t \mathbf{e}_t \otimes \mathbf{e}_t + \gamma_l \mathbf{e}_l \otimes \mathbf{e}_l + \gamma_n \mathbf{e}_n \otimes \mathbf{e}_n \tag{41}$$

where  $\mathbf{e}_t = \mathbf{e}_\theta$ ,  $\mathbf{e}_l = \mathbf{e}_l \times \mathbf{e}_n$ , and

$$\gamma_t = \frac{1}{2} \ln [u_{3,s}^2 + (1 + u_{s,s})^2], \quad \gamma_l = \ln \left[ 1 + \frac{u_s}{s} \right], \quad \gamma_n = \ln \left[ 1 + \frac{\partial q}{\partial X_3} \right]. \tag{42}$$

**3.1. General Solution at Equilibrium**

The displacements  $u_s = u_s(s)$  and  $u_3 = u_3(s)$  are determined by extremizing the potential energy functional. Since there is no part of the boundary where the traction is prescribed,  $\partial\Omega_0^o = \emptyset$ . Hence, substituting (16) into (29),

$$U = \int_{\rho}^v 2\pi s H \left[ \frac{2\mu}{\lambda + 2\mu} \{ \lambda \gamma_t \gamma_l + (\lambda + \mu)(\gamma_t^2 + \gamma_l^2) \} \right] ds. \tag{43}$$

Next, substituting in the eigenvalues (42) yields a functional of the form

$$U(u_s, u_3; v) = \int_{\rho}^v f(s, u_s(s), u_{s,s}(s), u_3(s), u_{3,s}(s)) ds. \tag{44}$$

As a result of assuming an infinitesimally thin membrane, the function  $q$  only arises in  $\gamma_n$  and thus does not enter into the strain energy for plane stress problems.

The Euler–Lagrange differential equations for the functional (44) are

$$\frac{\partial f}{\partial u_s} - \frac{\partial}{\partial s} \left( \frac{\partial f}{\partial u_{s,s}} \right) = 0 \quad \text{and} \quad \frac{\partial f}{\partial u_3} - \frac{\partial}{\partial s} \left( \frac{\partial f}{\partial u_{3,s}} \right) = 0. \tag{45}$$

After some manipulation, the combined differential equations furnish two second-order ordinary differential equations

$$u_{s,ss} - g_s(s, u_s, u_{s,s}, u_3, u_{3,s}) = 0 \quad \text{and} \quad u_{3,ss} - g_3(s, u_s, u_{s,s}, u_3, u_{3,s}) = 0, \tag{46}$$

where

$$\begin{aligned} g_s = & \{ 2 [ \lambda^2 \gamma_l^2 + 2\gamma_t(\lambda + \mu)(-\lambda + 2\gamma_t(\lambda + \mu)) + \gamma_l\lambda(-\lambda + 4\gamma_t(\lambda + \mu)) ] u_s \\ & \times (1 + u_{s,s}) + s [ (4\gamma_l^2\lambda(\lambda + \mu) + 2\gamma_t(-2 + 2\gamma_t)\lambda(\lambda + \mu) + \gamma_l(-8(\lambda + \mu)^2 \\ & + 2\gamma_t(5\lambda^2 + 8\lambda\mu + 4\mu^2)) u_{3,s}^2 - (\gamma_l\lambda + 2\gamma_t(\lambda + \mu))(1 + u_{s,s}) \\ & \times ((2\gamma_l - 2\gamma_t)(\lambda + 2\mu) + ((-2\gamma_t)\lambda + 4\gamma_l(\lambda + \mu))u_{s,s}) ] \} \\ & / \{ 2s (\gamma_l^2\lambda^2 + 2\gamma_t(-1 + 2\gamma_t)\lambda(\lambda + \mu) + 2\gamma_t(-2 + 2\gamma_t)(\lambda + \mu)^2) (s + u_s) \} \end{aligned}$$

and

$$\begin{aligned} g_3 = & \{ u_{3,s} [ (\lambda^2 \gamma_l^2 + 2\gamma_t(\lambda + \mu)(-\lambda + 2\gamma_t(\lambda + \mu)) + \gamma_l\lambda(-\lambda + 4\gamma_t(\lambda + \mu)) ] u_s \\ & + s (-\gamma_l^2\lambda(3\lambda + 4\mu) + 2\gamma_t(\lambda + \mu)(\lambda + 2\gamma_t\mu) + \gamma_l(4(\lambda + \mu)^2 \\ & - 2\gamma_t(3\lambda^2 + 6\lambda\mu + 4\mu^2)) - (4\gamma_l^2\lambda(\lambda + \mu) + 2\gamma_t(-2 + 2\gamma_t)\lambda(\lambda + \mu) \\ & + \gamma_l(-1 + 2\gamma_t)(5\lambda^2 + 8\lambda\mu + 4\mu^2))u_{s,s} ] \} / \{ s (\gamma_l^2\lambda^2 + 2\gamma_t(-1 + 2\gamma_t) \\ & \times \lambda(\lambda + \mu) + 2\gamma_t(-2 + 2\gamma_t)(\lambda + \mu)^2) (s + u_s) \}. \end{aligned}$$

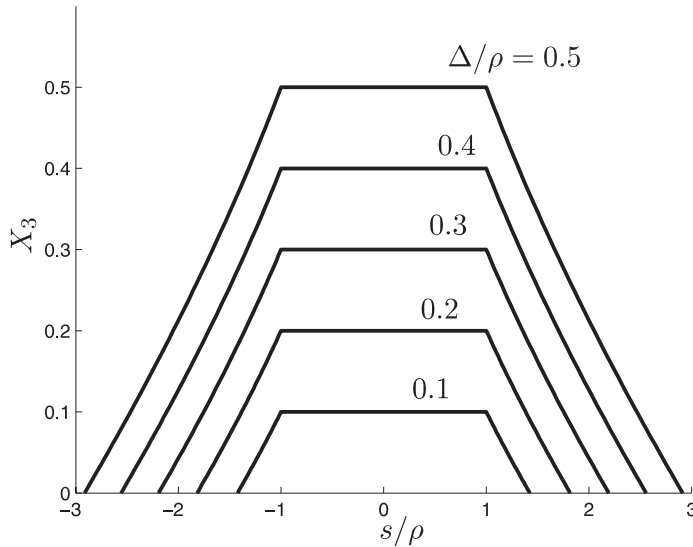


Figure 3. Profile of membrane for non-dimensional work of adhesion  $W_{ad}/E\rho = 10^{-5}$  and various shaft heights.

### 3.2. Boundary Conditions

The membrane is subject to the boundary conditions

$$u_s(\rho) = u_s(v) = u_3(v) = 0 \quad \text{and} \quad u_3(\rho) = \Delta. \tag{47}$$

These four boundary conditions are used to solve for the four constants of integration derived from (46). The remaining unknown is the radius  $v$  of the delaminated zone. From the Griffith energy balance, it follows that  $dU/dv = -dW_s/dv$ , where  $W_s$  is the work required to create new surface. Following from (36),  $W_s$  is given by

$$W_s = (\pi v^2 - \pi \rho^2) W_{ad}. \tag{48}$$

The energy release rate  $dU/dv$  is determined with the aid of Leibniz' rule:

$$\frac{dU}{dv} = f(v) + \int_{\rho}^v \left\{ \frac{\partial f}{\partial u_s} \frac{\partial u_s}{\partial v} + \frac{\partial f}{\partial u_{s,s}} \frac{\partial u_{s,s}}{\partial v} + \frac{\partial f}{\partial u_3} \frac{\partial u_3}{\partial v} + \frac{\partial f}{\partial u_{3,s}} \frac{\partial u_{3,s}}{\partial v} \right\} ds. \tag{49}$$

For stationary functions  $u_s$  and  $u_3$  satisfying (45), the integrand is the derivative of [25]

$$\frac{\partial f}{\partial u_{s,s}} \frac{\partial u_s}{\partial v} + \frac{\partial f}{\partial u_{3,s}} \frac{\partial u_3}{\partial v} \tag{50}$$

and so

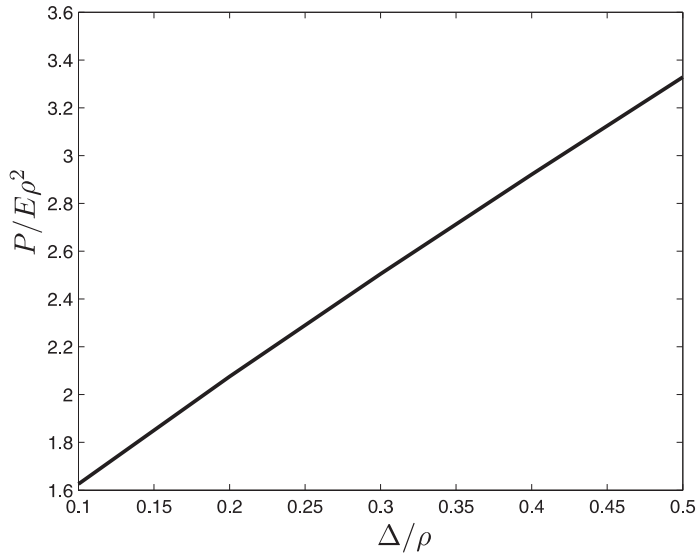


Figure 4. Non-dimensional normal load versus normalized shaft height for non-dimensional work of adhesion  $W_{ad}/E\rho = 10^{-5}$ .

$$\frac{dU}{dv} = f(v) + \left[ \frac{\partial f}{\partial u_{s,s}} \frac{\partial u_s}{\partial v} + \frac{\partial f}{\partial u_{3,s}} \frac{\partial u_3}{\partial v} \right]_v. \quad (51)$$

Noting that  $(\partial u_s/\partial v)_p = (\partial u_3/\partial v)_p = 0$ ,  $(\partial u_s/\partial v)_v = -u_{s,s}(v)$  and  $(\partial u_3/\partial v)_v = -u_{3,s}(v)$ , the energy release rate reduces to

$$\frac{dU}{dv} = f(v) - \left( \frac{\partial f}{\partial u_{s,s}} \right)_{s=v} u_{s,s}(v) - \left( \frac{\partial f}{\partial u_{3,s}} \right)_{s=v} u_{3,s}(v). \quad (52)$$

Thus, the Griffith energy balance yields an additional boundary condition

$$f(v) - \left( \frac{\partial f}{\partial u_{s,s}} \right)_{s=v} u_{s,s}(v) - \left( \frac{\partial f}{\partial u_{3,s}} \right)_{s=v} u_{3,s}(v) = -2\pi v W_{ad}, \quad (53)$$

which may be used to solve for  $v$ . This boundary condition is related to the second Weierstrass–Erdmann corner condition as well as the material (configurational) force balance at the edge of a delamination zone.

#### 4. SHAFT ROTATION

Now consider a rotation  $\psi \mathbf{e}_2$  about the pivot point  $\mathbf{p} = \rho \mathbf{e}_1$ , as shown in Figure 5. Hence, for  $\theta \in [0, 2\pi]$ ,

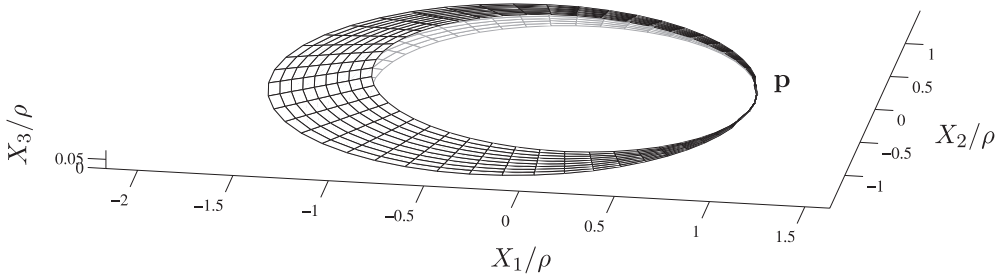


Figure 5. Delamination of membrane under shaft rotation of  $\psi = 0.05$  radians; non-dimensional work of adhesion  $W_{ad}/E\rho = 10^{-5}$ .

$$\mathbf{x} = \rho \mathbf{e}_s + \rho(1 - \cos \theta)(1 - \cos \psi) \mathbf{e}_1 + \rho(1 - \cos \theta) \sin \psi \mathbf{e}_3 \tag{54}$$

on  $\partial B$ .

For this system,  $\Omega$  is not axisymmetric and the task of determining the deformation at equilibrium is far more difficult than for the previous, axisymmetric system. Instead, approximate upper and lower bounds are obtained by employing the principles of minimum potential and maximum complementary energy, respectively.

#### 4.1. Upper Bound

To obtain an approximate expression for the potential energy it is assumed that

$$\mathbf{u}_0(s, \theta) = u_1(s, \theta) \mathbf{e}_1 + u_3(s, \theta) \mathbf{e}_3 \tag{55}$$

with

$$\begin{aligned} u_1(s, \theta) &= \rho(1 - \cos \theta)(1 - \cos \psi) \frac{v - s}{v - \rho} \\ u_3(s, \theta) &= \rho(1 - \cos \theta) \sin \psi \frac{v - s}{v - \rho}. \end{aligned}$$

Noting that  $\mathbf{e}_1 = \cos \theta \mathbf{e}_s - \sin \theta \mathbf{e}_\theta$ ,  $\mathbf{u}_0$  may be expressed as

$$\mathbf{u}_0(s, \theta) = u_1 \cos \theta \mathbf{e}_s - u_1 \sin \theta \mathbf{e}_\theta + u_3 \mathbf{e}_3. \tag{56}$$

This implies that  $\Omega$  is a ruled surface with directrix  $\partial B$ . To demonstrate this, consider any line along  $\mathbf{e}_s$  that is fixed to  $\Omega_0$ . Following from the linearity of  $u_1$  and  $u_3$ , such a line maps to a ruling on  $\Omega$ .

Based on the constitutive law and plane stress condition, it should be possible to derive  $q$  corresponding to the deformation associated with (55). However, for demonstration purposes, it is convenient to prescribe  $q = 0$ . This additional restriction on  $\mathcal{F}$ , though kine-

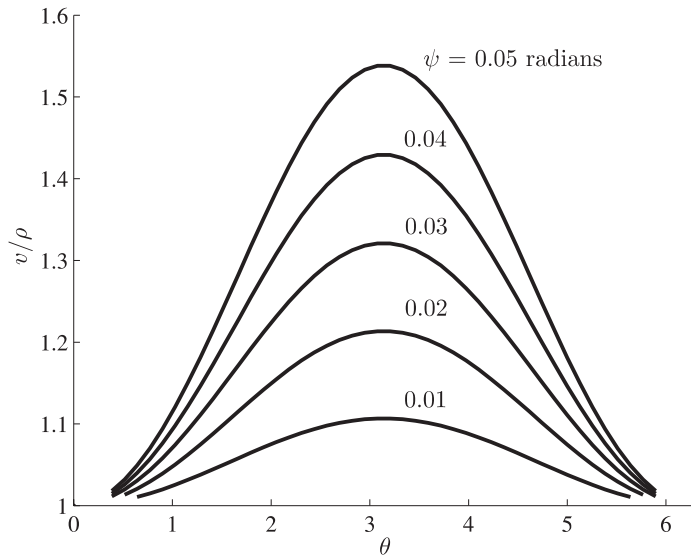


Figure 6. Plot of delamination zone for non-dimensional work of adhesion  $W_{ad}/E\rho = 10^{-5}$  and various angles of rotation.

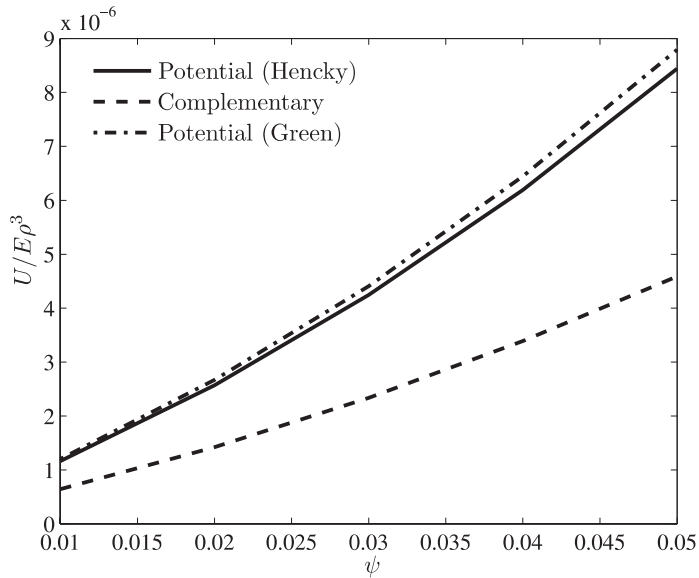


Figure 7. Plot of energy versus angle of rotation for non-dimensional work of adhesion  $W_{ad}/E\rho = 10^{-5}$ .

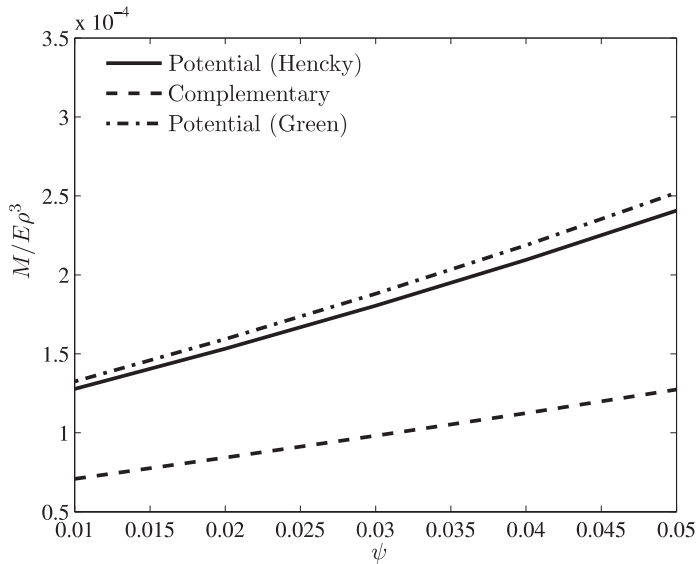


Figure 8. Plot of non-dimensional moment  $M/E\rho^3$  versus angle of rotation for non-dimensional work of adhesion  $W_{ad}/E\rho = 10^{-5}$ .

matically admissible, conflicts with the solution for plane stress and so is likely to reduce the accuracy of the upper bound approximation.

Evaluating  $\mathbf{e}_n$  from (9) and substituting  $\mathbf{u}_0$ ,  $\mathbf{e}_n$ , and  $q = 0$  into (27) yields the deformation gradient  $\mathbf{F}_m$  for points on the midplane. The corresponding strain tensor  $\mathbf{E}_m$  is then determined from (28) and substituted into (22) to determine the strain energy density,  $W$ . Lastly, by (29),

$$U = \int_0^{2\pi} \int_\rho^{v(\theta)} W H s ds d\theta. \tag{57}$$

The potential can also be evaluated for small strains (but large rotations) with Green’s strain tensor

$$\mathbf{E}_G = \frac{1}{2} (\mathbf{F}^T \mathbf{F} - \mathbf{I}). \tag{58}$$

**4.2. Lower Bound**

For the construction of a lower bound, the simplifying assumption of a ruled surface is not needed. Instead, it is assumed that the Piola stress tensor has the form

$$\mathbf{P} = \sigma_s \mathbf{e}_s \otimes \mathbf{e}_s + \sigma_\theta \mathbf{e}_\theta \otimes \mathbf{e}_\theta - \tau \mathbf{e}_s \otimes \mathbf{e}_3. \tag{59}$$

The eigenvalues of  $\mathbf{PP}^T$  are  $\sigma_s^2 + \tau^2$  and  $\sigma_\theta^2$ . Hence, following the arguments presented in Section 2.2, the Biot stresses are

$$t_t = \sqrt{\sigma_s^2 + \tau^2} \quad \text{and} \quad t_l = \sigma_\theta. \tag{60}$$

It is also convenient to let the ratio of  $t_t$  to  $t_l$  equal Poisson’s ratio. Hence, (60) implies

$$\sigma_\theta = \frac{\lambda}{2(\lambda + \mu)} \sqrt{\sigma_s^2 + \tau^2}. \tag{61}$$

As with (59), such a condition may conflict with kinematically admissible solutions to the constitutive equations for plane stress. Thus, setting  $t_t/t_l$  equal to Poisson’s ratio will likely reduce the accuracy of the lower bound approximation for  $U^*$ .

At equilibrium,  $\text{Div } \mathbf{P} = \mathbf{0}$ , which implies<sup>3</sup>

$$\frac{\partial \sigma_s}{\partial s} = \frac{1}{s}(\sigma_\theta - \sigma_s) \quad \text{and} \quad \frac{\partial \tau}{\partial s} = -\frac{\tau}{s}. \tag{62}$$

Substituting  $\sigma_\theta$  with (61) and solving,

$$\sigma_s = \frac{1}{4}C_1 s^{-\frac{\lambda+2\mu}{2(\lambda+\mu)}} - \frac{C_2^2}{C_1} s^{-\frac{3\lambda+2\mu}{2(\lambda+\mu)}} \quad \text{and} \quad \tau = \frac{C_2}{s}, \tag{63}$$

where  $C_1$  and  $C_2$  are constants of integration. These are used to evaluate the Biot stresses, which are then substituted into (24) and (25) to obtain  $\gamma_t$  and  $\gamma_l$ , respectively. Noting that  $\gamma_l = 0$ , the expression for strain energy reduces to

$$W = \frac{\lambda + 2\mu}{8\mu(\lambda + \mu)} t_t^2. \tag{64}$$

The complementary density is evaluated by substituting  $t_t, t_l = \lambda t_t / 2(\lambda + \mu), \gamma_t, \gamma_l = 0$  and  $W$  into (32), which yields  $W_c = w_c(s; C_1, C_2)$ .

For  $\theta \in [0, 2\pi]$ , the prescribed vectors in (30) are  $\mathbf{N}(v) = \mathbf{e}_s, \xi(v) = v\mathbf{e}_s, \mathbf{N}(\rho) = -\mathbf{e}_s,$  and  $\xi(\rho) \in \mathcal{B}$  such that

$$\xi(\rho) = \rho\mathbf{e}_s + \rho(1 - \cos \theta)(1 - \cos \psi)\mathbf{e}_1 + \rho(1 - \cos \theta) \sin \psi \mathbf{e}_3. \tag{65}$$

Hence, the total complementary energy is

$$\Phi = \int_0^{2\pi} \eta(\theta; C_1, C_2) H \, d\theta, \tag{66}$$

where

$$\eta = \rho^2(1 - \cos \theta)[(\tau)_\rho \sin \psi - (\sigma_s)_\rho(1 - \cos \psi) \cos \theta] + \int_\rho^v \left[ \frac{d}{ds} (s^2 \sigma_s) - s w_c \right] ds. \quad (67)$$

A lower bound on the strain energy is obtained by integrating the supremum of  $\eta H$  over  $C_1 \in \mathbb{R}$  and  $C_2 \in \mathbb{R}$  at each  $\theta \in [0, 2\pi]$ :

$$\Phi^{**} = \int_0^{2\pi} \max_{C_1, C_2} \eta H \, d\theta. \quad (68)$$

**4.3. Approximate Solution at Equilibrium**

The strain energy density  $W$  is approximated by (22) evaluated with Green’s strain tensor. Integrating  $WHs$  over  $s \in [\rho, v]$  in (57) yields a functional of the form

$$U = \int_0^{2\pi} h(\theta, v(\theta)) \, d\theta, \quad (69)$$

where

$$\begin{aligned} h = & \{ H \rho^2 (-10 v^4 \lambda - 24 v^4 \mu + 16 v^3 \mu \rho + 14 v^2 \lambda \rho^2 + 4 v^2 \mu \rho^2 + 16 v \mu \rho^3 \\ & - 4 \lambda \rho^4 - 12 \mu \rho^4 + 3 v^4 \lambda \cos(3\theta) + 6 v^4 \mu \cos(3\theta) - 3 v^2 \lambda \rho^2 \cos(3\theta) \\ & - 6 v^2 \mu \rho^2 \cos(3\theta) + 4 v^4 \lambda \ln(v) + 12 v^4 \mu \ln(v) + 16 v^3 \lambda \rho \ln(v) \\ & + 24 v^3 \mu \rho \ln(v) + 12 v^2 \lambda \rho^2 \ln(v) + 28 v^2 \mu \rho^2 \ln(v) - 2 v^4 \lambda \cos(3\theta) \ln(v) \\ & - 2 v^4 \mu \cos(3\theta) \ln(v) - 4 v^3 \lambda \rho \cos(3\theta) \ln(v) - 12 v^3 \mu \rho \cos(3\theta) \ln(v) \\ & - 2 v^2 \lambda \rho^2 \cos(3\theta) \ln(v) - 2 v^2 \mu \rho^2 \cos(3\theta) \ln(v) - 4 v^4 \lambda \ln(\rho) - 12 v^4 \mu \ln(\rho) \\ & - 16 v^3 \lambda \rho \ln(\rho) - 24 v^3 \mu \rho \ln(\rho) - 12 v^2 \lambda \rho^2 \ln(\rho) - 28 v^2 \mu \rho^2 \log(\rho) \\ & + 2 v^4 \lambda \cos(3\theta) \log(\rho) + 2 v^4 \mu \cos(3\theta) \ln(\rho) + 4 v^3 \lambda \rho \cos(3\theta) \ln(\rho) \\ & + 12 v^3 \mu \rho \cos(3\theta) \ln(\rho) + 2 v^2 \lambda \rho^2 \cos(3\theta) \ln(\rho) + 2 v^2 \mu \rho^2 \cos(3\theta) \ln(\rho) \\ & + \cos(\theta) (-(v - \rho) (v^3 (7 \lambda + 26 \mu) + v^2 (15 \lambda + 2 \mu) \rho + 4 v (3 \lambda + 11 \mu) \rho^2 \\ & + 4 (\lambda + \mu) \rho^3)) + 2 v^2 (v^2 (\lambda + 5 \mu) + 2 v (\lambda - \mu) \rho + (\lambda + 5 \mu) \rho^2) \ln(v) \\ & - 2 v^2 (v^2 (\lambda + 5 \mu) + 2 v (\lambda - \mu) \rho + (\lambda + 5 \mu) \rho^2) \ln(\rho) \\ & - 2 v \cos(2\theta) (-(v - \rho) (v^2 (7 \lambda + 10 \mu) + v (11 \lambda + 30 \mu) \rho + 4 (\lambda + \mu) \rho^2)) \\ & + 2 v (v^2 (\lambda + \mu) + 2 v (2 \lambda + 5 \mu) \rho + (3 \lambda + 5 \mu) \rho^2) \log(v) - 2 v (v^2 (\lambda + \mu) \\ & + 2 v (2 \lambda + 5 \mu) \rho + (3 \lambda + 5 \mu) \rho^2) \ln(\rho)) \sin(\theta/2)^2 \sin(\psi/2)^4 \} / \{ 2 (v - \rho)^4 \}. \end{aligned}$$

The work required to create new surface is given by

$$W_s = \int_0^{2\pi} \int_\rho^{v(\theta)} W_{ad} s \, ds \, d\theta. \quad (70)$$

Thus, the total energy of the system is

$$E = U + W_s = \int_0^{2\pi} \left\{ h + \frac{v^2 - \rho^2}{2} W_{ad} \right\} d\theta. \quad (71)$$

By the Griffith energy balance,  $E$  is stationary at equilibrium. Hence the integrand of  $E$  satisfies the Euler–Lagrange differential equation, which implies

$$\frac{\partial h}{\partial v} + v W_{ad} = 0. \quad (72)$$

Substituting the expression for  $h$ , (72) may be expressed as

$$\begin{aligned} 0 = & v W_{ad}(v - \rho)^5 + H\rho^2(2v^4\lambda + 6v^4\mu + 26v^3\lambda\rho + 46v^3\mu\rho - 16v^2\lambda\rho^2 \\ & - 26v^2\mu\rho^2 - 20v\lambda\rho^3 - 42v\mu\rho^3 + 8\lambda\rho^4 + 16\mu\rho^4 - v^4\lambda \cos(3\theta) \\ & - v^4\mu \cos(3\theta) - 7v^3\lambda\rho \cos(3\theta) - 17v^3\mu\rho \cos(3\theta) + 4v^2\lambda\rho^2 \cos(3\theta) \\ & + 11v^2\mu\rho^2 \cos(3\theta) + 4v\lambda\rho^3 \cos(3\theta) + 7v\mu\rho^3 \cos(3\theta) - 16v^3\lambda\rho \ln(v) \\ & - 36v^3\mu\rho \ln(v) - 36v^2\lambda\rho^2 \ln(v) - 64v^2\mu\rho^2 \ln(v) - 12v\lambda\rho^3 \ln(v) \\ & - 28v\mu\rho^3 \ln(v) + 6v^3\lambda\rho \cos(3\theta) \ln(v) + 10v^3\mu\rho \cos(3\theta) \ln(v) \\ & + 8v^2\lambda\rho^2 \cos(3\theta) \ln(v) + 20v^2\mu\rho^2 \cos(3\theta) \ln(v) + 2v\lambda\rho^3 \cos(3\theta) \ln(v) \\ & + 2v\mu\rho^3 \cos(3\theta) \ln(v) + 16v^3\lambda\rho \ln(\rho) + 36v^3\mu\rho \ln(\rho) + 36v^2\lambda\rho^2 \ln(\rho) \\ & + 64v^2\mu\rho^2 \ln(\rho) + 12v\lambda\rho^3 \ln(\rho) + 28v\mu\rho^3 \ln(\rho) - 6v^3\lambda\rho \cos(3\theta) \ln(\rho) \\ & - 10v^3\mu\rho \cos(3\theta) \ln(\rho) - 8v^2\lambda\rho^2 \cos(3\theta) \ln(\rho) - 20v^2\mu\rho^2 \cos(3\theta) \ln(\rho) \\ & - 2v\lambda\rho^3 \cos(3\theta) \ln(\rho) - 2v\mu\rho^3 \cos(3\theta) \ln(\rho) + \cos(\theta)((v - \rho)(v^3(\lambda + 5\mu) \\ & + v(28\lambda + 51\mu)\rho^2 + 4(3\lambda + 7\mu)\rho^3 + v^2(20\lambda\rho + 38\mu\rho)) \\ & - 2v\rho(3v^2(\lambda + 3\mu) + 2v(2\lambda + \mu)\rho + (\lambda + 5\mu)\rho^2) \ln(v) \\ & + 2v\rho(3v^2(\lambda + 3\mu) + 2v(2\lambda + \mu)\rho + (\lambda + 5\mu)\rho^2) \ln(\rho)) \\ & - 2\cos(2\theta)((v - \rho)(v^3(\lambda + \mu) + 20v^2(\lambda + 2\mu)\rho + 3v(6\lambda + 13\mu)\rho^2 \\ & + 2(\lambda + \mu)\rho^3) - 2v\rho(v^2(4\lambda + 7\mu) + v(9\lambda + 20\mu)\rho + (3\lambda + 5\mu)\rho^2) \ln(v) \\ & + 2v\rho(v^2(4\lambda + 7\mu) + v(9\lambda + 20\mu)\rho + (3\lambda + 5\mu)\rho^2) \ln(\rho)) \sin(\theta/2)^2 \sin(\psi/2)^4. \end{aligned}$$

Solving (72) yields the approximate shape  $v^{**} = v^{**}(\theta)$  of the delamination zone at equilibrium. Substituting this solution into (55) leads to the deformed configuration of the membrane for a prescribed angle of rotation,  $\psi$ . The corresponding strain energy is

$$U^{**} = \int_0^{2\pi} h(\theta, v^{**}(\theta)) d\theta. \tag{73}$$

Following the arguments in Section 2.4,  $U^{**}$  is an upper bound approximation of the strain energy  $U^*$  at equilibrium.

**5. NUMERICAL RESULTS AND DISCUSSION**

The boundary value problem formed by the differential equations (46) and boundary conditions (47) are solved in Matlab 7.0 (The Mathworks, Inc. 2004) using a finite difference method. The initial guess for functions  $u_s(s)$  and  $u_3(s)$  are

$$(u_s)_{init} = 0 \quad \text{and} \quad (u_3)_{init} = \Delta \frac{v - s}{v - p}. \tag{74}$$

Figure 3 is a side-view (not to scale) of the membrane for  $W_{ad}/E\rho = 10^{-5}$ , where  $E = (3\lambda\mu + 2\mu^2)/(\lambda + \mu)$  is the elastic modulus,  $H/\rho = 0.01$ , and Poisson’s ratio  $\lambda/2(\lambda + \mu) = 0.4$ . The difference between the shaft and delamination zone radii is observed to increase nearly linearly with shaft height. The load necessary to achieve a prescribed height is obtained by evaluating

$$P = \frac{dU}{d\Delta} \tag{75}$$

(see Figure 4).

Numerical results for the case of shaft rotation are presented in Figures 6–8. Again,  $W_{ad}/E\rho = 10^{-5}$ ,  $H/\rho = 0.01$ , and  $\lambda/2(\lambda + \mu) = 0.4$ . An algebraic expression for (72) is obtained with the aid of Mathematica 4 (Wolfram Research, Inc. 2000) and is solved for  $v = v(\theta)$  by using a scalar root finder in Matlab (see Figure 6). Equation (72) is derived from Green’s strain tensor (58), which is a small strain approximation of the Hencky strain (13). For the geometries considered here, both strain tensors yield similar upper bounds for the elastic strain energies, as demonstrated in Figure 7. Hencky strain is also used to approximate the maximum complementary energy, which furnishes a lower bound on the elastic energy. The tightness of these bounds indicate the accuracy of the solution for  $v(\theta)$ . Evaluating the derivative of the energy approximations with respect to  $\psi$  yields the moment necessary to achieve a prescribed angle of rotation, i.e.

$$M = \frac{dU}{d\psi} \tag{76}$$

(see Figure 8).

## 6. CONCLUSION

The numerical results indicate that a pure membrane adhering to a flat resists both normal forces and moment when loaded at its center. Moreover, for the geometries considered here the resistance to delamination increases with the size of the delamination zone.

In closing, the current analysis demonstrates how stationary principles can be used to obtain bounds on an otherwise difficult membrane delamination problem, allowing for an analytic approximation with known accuracy. Future work will focus on the design of a bio-inspired dry adhesive that incorporates the spatular shape presented here. Predictions for resistance to normal and moment loads can be compared with other spatular shapes, such as those presented in [7].

## NOTES

1. Computed as  $\mathbf{F} = \mathcal{X} \otimes \nabla$ , where  $\nabla = \mathbf{e}_s \frac{\partial}{\partial s} + \mathbf{e}_\theta \frac{1}{s} \frac{\partial}{\partial \theta} + \mathbf{e}_3 \frac{\partial}{\partial X_3}$  [23].
2. Performed by taking the trace of both sides, substituting the solution for  $\text{trE}$  back into (18) and then solving for  $\mathbf{E}$ .
3. Computed as  $\text{Div } \mathbf{P} = \nabla \cdot \mathbf{P}$ .

*Acknowledgments.* The authors wish to thank the reviewers for their insightful comments and suggestions. This work was supported by NSF NIRT EEC-0304730, DARPA, a DCI Postdoctoral Fellowship (R. E. Groff), and the Emhart Corporation. Any opinions, findings and conclusions or recommendations expressed in this material are those of the authors and do not necessarily reflect the views of the National Science Foundation (NSF).

## REFERENCES

- [1] Malyshev, B. M. and Salganik, R. L. *International Journal of Fracture Mechanics*, 1, 114 (1965).
- [2] Williams, J. G. *International Journal of Fracture*, 87, 265–288 (1997).
- [3] Wan, K.-T. and Mai, Y.-W. *International Journal of Fracture*, 74, 181–197 (1995).
- [4] Wan, K.-T. and Kogut, L. *Journal of Micromechanical Microengineering*, 15, 778–784 (2005).
- [5] Shenoy, V. B. and Freund, L. B. *Proceedings of the National Academy of Sciences of the USA*, 102, 3213–3218 (2005).
- [6] Persson, B. N. J. and Gorb, S. *Journal of Chemical Physics*, 119, 11437–11444 (2003).
- [7] Spolenak, R., Gorb, S., Gao, H. and Arzt, E. *Proceedings of the Royal Society A*, 461, 305–319 (2004).
- [8] Huber, G., Mantz, H., Spolenak, R., Mecke, K., Jacovs, K., Gorb, S. N., Arzt, E. *Proceedings of the National Academy of Sciences of the USA*, 102, 16293–16296 (2005).
- [9] Hansen, W. R. and Autumn, K. *Proceedings of the National Academy of Sciences of the USA*, 102, 385–389 (2004).
- [10] Autumn, K. *American Scientist*, 24, 124–132 (Mar–Apr 2006).
- [11] Kahn, J. *National Geographic*, 209, 98–119 (June 2006).
- [12] Autumn, K., Sitti, M., Liang, Y. A., Peattie, A. M., Hansen, W. R., Sponberg, S., Kenny, T. W., Fearing, R., Israelachvili, J. N. and Full, R. J. *Proceedings of the National Academy of Sciences of the USA*, 99, 12252–12256 (2002).
- [13] Kendall, K. *Journal of Physics D: Applied Physics*, 4, 1186–1195 (1971).
- [14] Haddow, J. B., Favre, L. and Ogden, R. W. *Journal of Engineering Mathematics*, 37, 65–84 (2000).
- [15] Koiter, W. T. *Trends in Applications of Pure Mathematics to Mechanics*, 1, 207–232 (1976).
- [16] Liu, S., Haddow, J. B. and Dost, S. *Acta Mechanica*, 99, 191–200 (1993).
- [17] Steigmann, D. J. *International Journal of Non-linear Mechanics*, 40, 255–270 (2005).
- [18] Ogden, R. W. *Non-linear Elastic Deformations*, Ellis Horwood, Chichester, 1984.

- [19] Valid, R. *The Nonlinear Theory of Shells through Variational Principles*, Wiley, New York, 1995.
- [20] Gao, D. Y. *Duality Principles in Nonconvex Systems*, Kluwer, Dordrecht, 2000.
- [21] Anand, L. *Journal of Applied Mechanics*, 46, 78–82 (1979).
- [22] Anand, L. *Journal of Mechanics and Physics of Solids*, 34, 293–304 (1986).
- [23] Bertram, A. *Elasticity and Plasticity of Large Deformations*, Springer, Berlin, 2000.
- [24] Anderson, T. L. *Fracture Mechanics*, 3rd edition, CRC/Taylor and Francis, Boca Raton, FL, 29 (2005).
- [25] Troutman, J. L. *Variational Calculus and Optimal Control*, 2nd edition, Springer, New York, 1996.
- [26] Carbone, G., Mangialardi, L. and Persson, B. N. J. *Physical Review B*, 70, 125407 (2004).